SCIENTIFIC REPORTS
nature research

OPEN

Gate-tunable graphene-based Hall sensors on flexible substrates with increased sensitivity

Burkay Uzlu[1,2*], Zhenxing Wang[1], Sebastian Lukas[1,2], Martin Otto[1], Max C. Lemme[1,2] & Daniel Neumaier[1]

We demonstrate a novel concept for operating graphene-based Hall sensors using an alternating current (AC) modulated gate voltage, which provides three important advantages compared to Hall sensors under static operation: (1) The sensor sensitivity can be doubled by utilizing both n- and p-type conductance. (2) A static magnetic field can be read out at frequencies in the kHz range, where the 1/f noise is lower compared to the static case. (3) The off-set voltage in the Hall signal can be reduced. This significantly increases the signal-to-noise ratio compared to Hall sensors without a gate electrode. A minimal detectable magnetic field B_{min} down to 290 nT/√Hz and sensitivity up to 0.55V/VT was found for Hall sensors working on flexible polyimide (PI) substrates. This clearly outperforms state-of-the-art flexible Hall sensors and is comparable to the values obtained by the best rigid III/V semiconductor Hall sensors.

Magnetic field sensors are widely used in several key industries such as consumer electronics, automotive, healthcare and robotics[1,2], where they provide position and speed detection, switching applications or current monitoring[3]. Hall effect sensors currently dominate the market in terms of these operations[4–8] and the key figures of merit for these sensors are their magnetic field resolution (B_{min}) and current (S_i) and voltage related (S_v) sensitivities[9]. Today's technology utilizes mainly silicon based Hall sensors because of the advanced silicon CMOS technology that enables reliable and cost efficient production[10]. However, applications of silicon based Hall sensors are limited by their relatively low sensitivity when compared to Hall sensors based on III/V semiconductors such as InAs and GaAs[11–13], and by their mechanical stiffness. Graphene, because of its very high mobility μ and low charge carrier density n ($S_v \sim \mu$ *and* $S_i \sim 1/n$) as well as its mechanical flexibility, appears to be ideally suited as the sensing material in Hall effect sensors[14–21]. Previously, graphene based Hall sensors were demonstrated, that outperformed silicon and other III/V semiconductors based rigid sensors[8,9,15,22–24]. In addition, graphene-based Hall sensors already significantly outperform all other technologies on flexible substrates[22]. However, the sensitivity of flexible graphene Hall sensors is not yet comparable to rigid Hall sensors based on conventional semiconductors, at least if the graphene Hall sensors are fabricated with a scalable approach.

In this work, we introduce a novel concept for increasing the signal-to-noise ratio in graphene-based Hall sensors with an AC modulated gate electrode, on flexible substrates with local top-gate. Such dynamic gating provides three advantages compared to graphene Hall sensors under static operation: First, the AC modulated gate voltage allows reaching sensitivity maxima for n- and p-type conductance, which doubles the effective sensitivity. This advantage is unique for graphene based Hall sensors due to their ambipolar operation. Second, a static magnetic field can be read out at higher frequencies, where 1/f noise is significantly lower. And third, offsets in the Hall voltage can be reduced by adjusting a static voltage superimposed on the AC voltage. The basic operation mechanism of such a top-gated Hall sensor is illustrated in Fig. 1a. While the second and third advantage can be achieved by other methods, *e.g.* AC modulation of the supply voltage for the former or spinning current readout for the latter[25], there exists no approach offering all three advantages. In the following, we describe the fabrication and detailed characterization of top-gated graphene Hall sensors on flexible substrates and demonstrate an increased signal-to-noise ratio. These Hall sensors do not only set a new benchmark for flexible Hall-sensors, but are also on a par with the best III-V based rigid Hall sensors.

[1]Advanced Microelectronic Center Aachen (AMICA), AMO GmbH, 52074, Aachen, Germany. [2]Chair of Electronic Devices, RWTH Aachen University, 52074, Aachen, Germany. *email: uzlu@amo.de

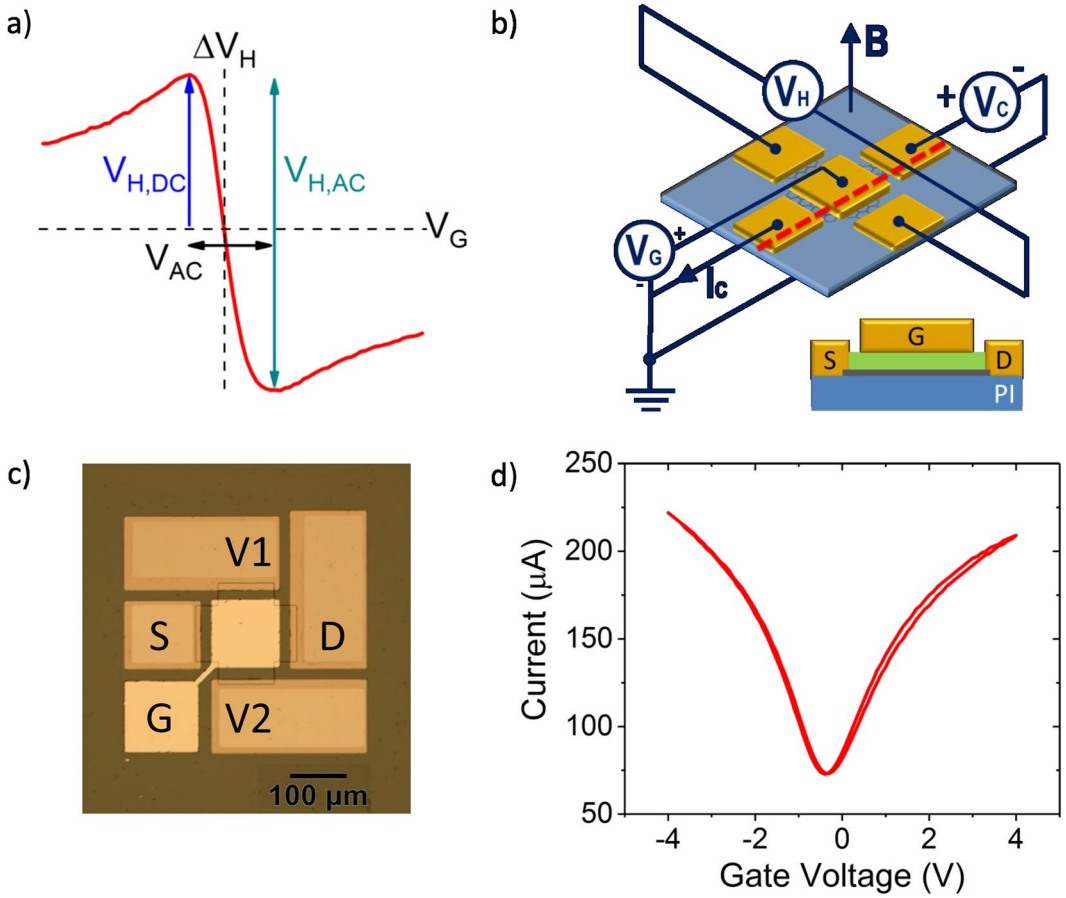

Figure 1. Device schematic and the I-V characteristics of the top gated graphene based flexible Hall sensor. (**a**) Comparison of measured ΔV_H and basic operating principles using a DC gate voltage and an AC modulated gate voltage across the charge neutrality point. In the latter, both sensitivity maxima for n- and p-type conductance can be utilized and the effective sensitivity is doubled by AC gate modulation. (**b**) Isometric device schematic of the top gated graphene Hall sensor with corresponding biasing scheme (top). Schematic illustration of the cross section along the red dashed line in the device schematic (bottom). Graphene and Al_2O_3 encapsulation are indicated in grey and green colors respectively. (**c**) Optical microscope image of a device after fabrication with four probing metal pads and top gate. A constant bias voltage V_C is applied between the contacts S and D and ΔV_H is measured between the contact V1 and V2. Gate voltage V_G is applied to the contact G. d) Room temperature two terminal top gate characteristic of the fabricated device at V_C of 300 mV.

Results and Discussion

Schematics and the optical microscope image of the fabricated Hall sensors on PI substrate are shown in Fig. 1b,c. The transfer characteristic of one representative device is shown in Fig. 1d for both sweeping directions from −4 V to 4 V and back. These field effect transistor measurements have been conducted to check the integrity and quality of the devices. The transfer characteristic shows little hysteresis, which demonstrates successful passivation by the Al_2O_3 [26], and also a low residual doping level of the graphene of $3.5 \cdot 10^{11}$ cm^{-2}. The two-probe field effect mobility of the device is 2830 cm^2/Vs, including the contact and access resistance. Detailed device statistics of 51 out of total 54 devices fabricated on the same chip are shown in the Supplementary Information and demonstrate good reproducibility. Three devices which did not function are excluded from the statistics.

First, conventional Hall effect measurements have been performed with constant gate voltage in order to extract the basic parameters of the device. The measurement configuration is shown in Fig. 1b. A constant bias voltage (V_C) and a magnetic field perpendicular to the graphene channel, ranging from 7.2 to 28.8 mT, has been applied and the current (I_C) and the Hall voltage (V_H) have been measured. In addition, the charge carrier concentration of the graphene, and thus the sensitivity of the device, has been controlled by applying a gate voltage (V_G). The offset removed Hall voltage ΔV_H, which represents the measured Hall voltage minus the offset voltage at zero magnetic field ($\Delta V_H = V_H - V_{H,B=0}$) is plotted as a function of gate voltage in Fig. 2a with a constant $V_C = 300$ mV. The voltage (S_v) and current related (S_i) sensitivities can be derived from this measurement using Eqs. (1) and (2) [15]:

$$S_v = \frac{1}{V_c}\left|\frac{\partial V_H}{\partial B}\right| \quad (1)$$

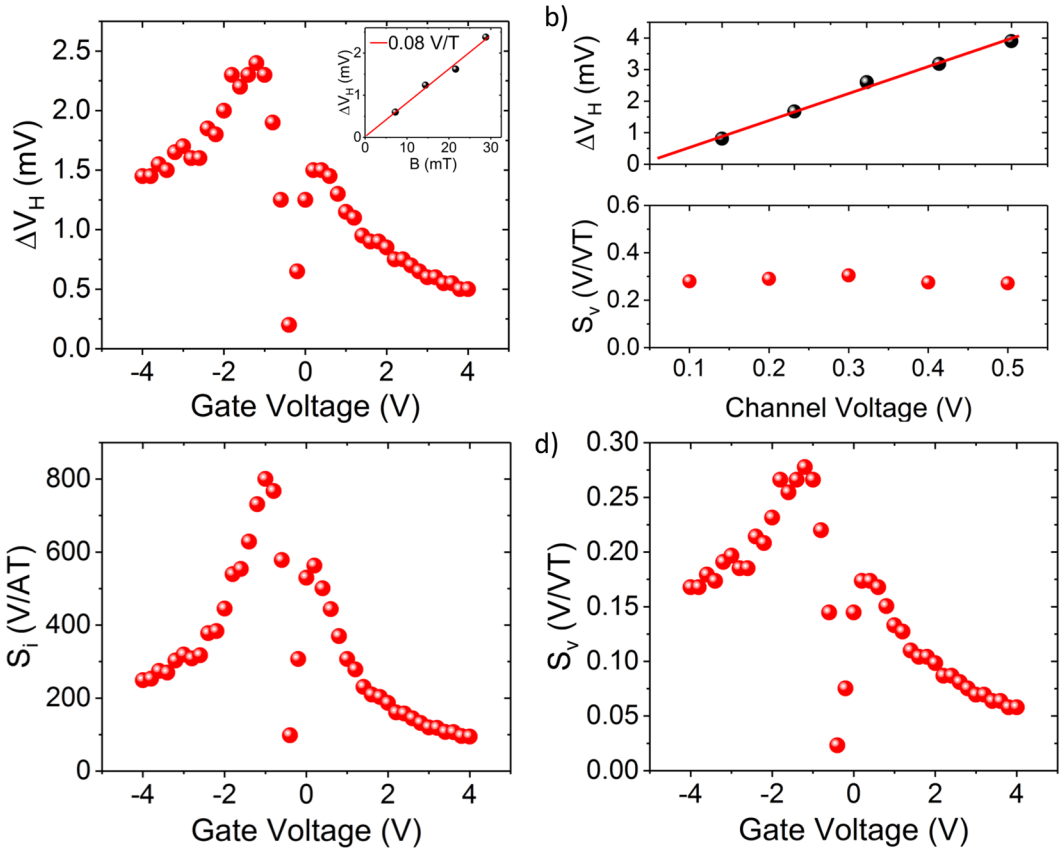

Figure 2. Hall measurements of the sensor. (**a**) Magnitude of the ΔV_H as a function of the gate voltage at $V_C = 300\,\text{mV}$. The inset shows ΔV_H as a function of the magnetic field at $V_G = -1.2\,\text{V}$. (**b**) ΔV_H and voltage sensitivity S_v as a function of channel voltage V_C. (**c,d**) Absolute values of current sensitivity S_i and S_v plotted against V_G at $V_C = 300\,\text{mV}$.

and

$$S_i = \frac{1}{I_c}\left|\frac{\partial V_H}{\partial B}\right| \tag{2}$$

Figures 2c,d show S_v and S_i as a function of top gate voltage at a bias voltage of $V_C = 300\,\text{mV}$. The sensitivities crucially depend on the doping level of the graphene with a slight asymmetry between hole and electron transport regime. The maximum values for the sensitivities S_i and S_v are found to be 800 V/AT and 0.278 V/VT, respectively, for this device. We further observe a linear dependence of ΔV_H regarding V_C (Fig. 2b), which indicates that the sensitivities are independent of the applied bias and the sensors can be operated with low power. The corresponding charge carrier mobility (μ) can be calculated according to Eq. (3)[9]:

$$\mu = S_v \frac{L}{W} \tag{3}$$

where L and W are the length and width of the graphene channel in the fabricated Hall sensor device. This results in a charge carrier mobility of 4400 cm^2/Vs at the S_v maxima, which turned out to be an average value across the chip. Detailed performance analyses of all devices on the chip are shown in Figs. S1 and S2 in the Supplementary Information. The device with the highest values on this chip showed $S_v = 0.35\,\text{V/VT}$, corresponding to a mobility of 5600 cm^2/Vs.

The characteristics of the Hall sensors under AC gate modulation have been measured in a different setup, illustrated in Fig. 3a. Here, we report data measured on the same device as discussed in Fig. 2. In this setup, a signal generator is used to modulate the gate voltage, which consists of a static offset voltage plus an AC voltage. An SRS 380 lock-in amplifier is used to demodulate the read-out signal (V_H). The modulation frequency is fixed at 2 kHz for all measurements, which is well below the calculated RC bandwidth of the Hall sensor of 1.7 MHz. Figure 3b shows the ΔV_H as a function of the peak-to-peak AC gate modulation amplitude. In this measurement a constant V_C of 300 mV was applied. As expected from the gate voltage dependent sensitivity, the Hall signal increases first with increasing AC amplitude and decreases again after reaching a maximum at ~1.5 V. To directly compare the Hall voltage under DC and AC operation, 45 s long measurements have been performed while the magnetic field was alternated between zero and values up to 28.8 mT (Fig. 3c). In both measurements,

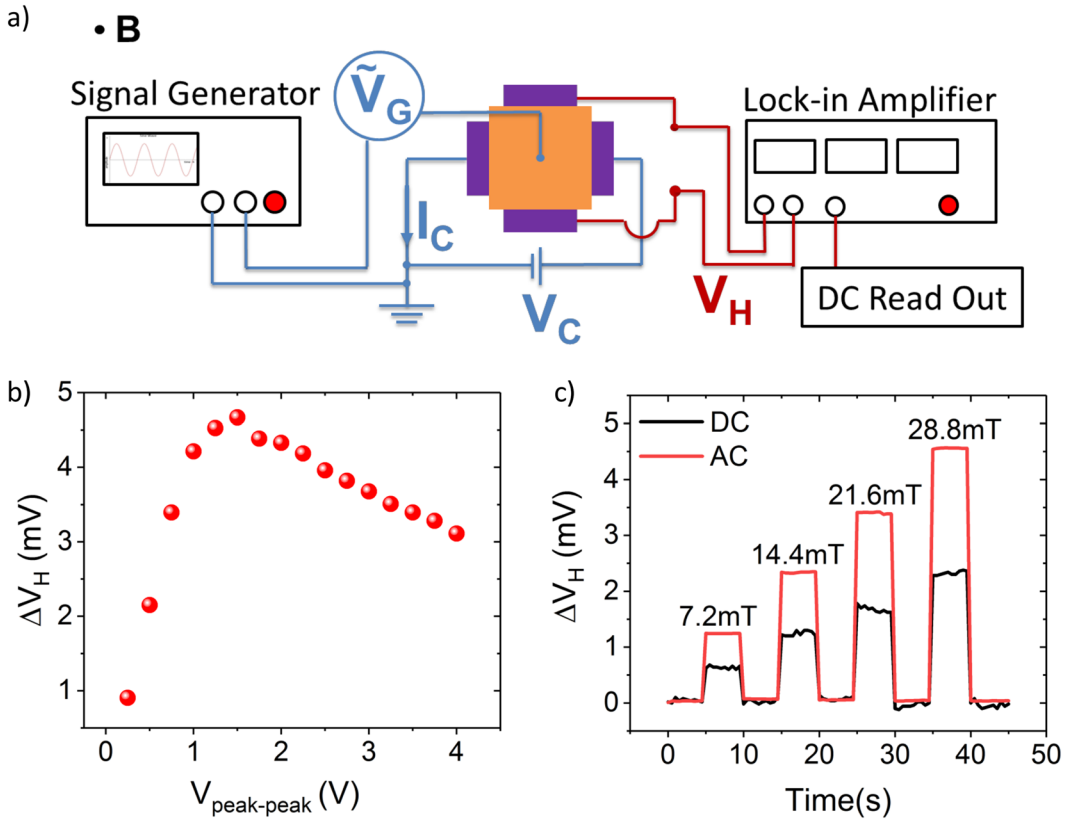

Figure 3. Hall measurements of the sensor with gate voltage modulation. (**a**) Illustration of AC gate modulation setup. A signal generator is used to modulate the gate voltage and an SRS 380 lock-in amplifier is used to demodulate the read-out signal (V_H). (**b**) Hall voltage response of the device to the varying magnetic field at a peak to peak gate modulation amplitude at 28.8 mT. (**c**) Offset removed Hall voltage under DC (black) and AC (red) operation over time, while the magnetic field was stepped between 7.2 mT up to 28.8 mT. For both measurements, V_C was 300 mV and the gate voltage was tuned to maximum sensitivity, i.e. $V_G = -1.2$ V for the DC measurement and $V_G = 1.5$ V for the AC case.

$V_C = 300$ mV. The gate voltages have been set to achieve maximum sensitivity, i.e. $V_G = -1.2$ V for the DC measurement and $V_G = 1.5$ V AC voltage in amplitude for the AC case. The effective Hall signal and thus the sensitivity is approximately a factor 2 higher for the AC case, confirming the advantage of the AC gate modulation. The extracted sensitivity S_v is 0.55 V/VT and 0.278 V/VT for the AC and DC case, respectively (Supplementary Information Fig. S3). In addition, the noise in the AC measurements is significantly lower compared to the DC case. However, we note that this noise reduction is mainly due to the sensor read-out using a lock-in amplifier for the AC case, which is not possible under static operation.

The magnetic resolution B_{min} represents another key parameter for Hall sensors in addition to the current and voltage related sensitivities. It can be calculated using the noise spectral density and the sensitivity of the sensor using Eq. (4) [15]:

$$B_{min} = \frac{\sqrt{P_v}}{(S_v \cdot V_c)} \tag{4}$$

The noise power spectral density (P_V) of the Hall voltage is measured in ambient with SR770 FFT Spectrum analyzer directly connected to the contacts V1 and V2 in Fig. 1c, while a constant bias voltage V_C between the contacts S and D and zero magnetic field B are applied[9]. Zero V_G is applied during the noise measurements since the harmonic contributions of the AC modulated gate restrains determining of the noise floor. However, contribution of the gate voltage to the noise is studied and analyzed in detail previously by Mavredakis *et al.*[27] and the effect of the noise originated from the gate bias on the B_{min} of the Hall sensor will not be significant. The results are shown in Fig. 4a, confirming that the major source of noise has a 1/f dependency for the measured frequency range up to 12 kHz. Hence, higher read-out frequencies lead to lower noise levels. The magnetic resolution is derived from P_V (Fig. 4b). At 2 kHz, B_{min} is found to be 500 nT/$\sqrt{\text{Hz}}$. The lowest value measured on the chip was 290 nT/$\sqrt{\text{Hz}}$. Comparison of our findings with literature values for the state-of-the-art Hall sensor elements made from silicon, graphene and other III/V based semiconductors on rigid and flexible substrates are shown in Table 1. The table clearly shows that our CVD graphene based Hall sensors on flexible substrates remarkably outperforms all the other Hall sensor elements on flexible substrates and are highly competitive with respect to all

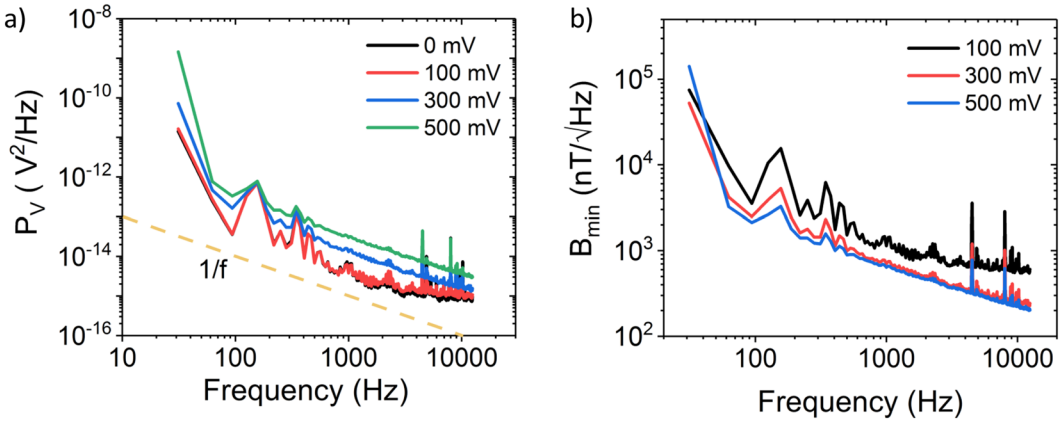

Figure 4. Noise and B_{min} measurements. (**a**) Noise power spectral density (P_V) as a function of frequency. The dashed line indicates 1/f behavior of the noise. (**b**) Derived magnetic resolution B_{min} of the Hall sensor as a function of frequency.

	Substrate	S_I (V/AT)	S_v (V/VT)	B_{min} (nT/$\sqrt{Hz}$)	Frequency (kHz)	Conditions
Si[1,29]	Rigid	100	0.1	5000	3	n/a
AlInSb[4,6]	Rigid	2750	2.2	58	1	Vacuum
GaAs[29]	Rigid	1100	n/a	800	3	n/a
Exfoliated Gr-hBN[9]	Rigid	4100	2.16	50	3	Vacuum
CVD Gr[30]	Rigid	800	n/a	500	3	Air
CVD Gr[15]	Rigid	2093	0.35	100	3	Air
CVD Gr[8]	Flexible	75	0.093	n/a	n/a	Air
CVD Gr-hBN[22]	Flexible	2270	0.68	n/a	n/a	Air
Bismuth[31]	Flexible	2.3	n/a	n/a	n/a	Air
This work	Flexible	1500	0.55	500	2	Air
This work (max)	Flexible	2580	0.68	290	2	Air

Table 1. Metrics comparison of different high-performance Hall elements working at room temperature. ('Gr' stands for graphene).

existing technologies on rigid substrate. The measured minimum magnetic resolution of our Hall sensors also outperform the state-of-the-art Hall elements based on Si and is close to the very best values achieved by AlInSb[4,6] and exfoliated graphene[9] based Hall sensors. It should be noted that the highest[9,22] values shown in the Table 1, have been achieved by non-scalable micro-mechanical exfoliated graphene and hBN and/or in vacuum conditions.

Finally, the stability of the devices for flexible applications has been investigated. Bending tests have been performed where the device was exposed to varying strain values. Figure 5a shows a photograph of a flexible chip after it has been peeled off mechanically from the silicon carrier substrate. For electrical measurements, the PI substrate has been bent under different bending radii of 25.4 mm, 12.7 mm, and 6.4 mm, respectively (Fig. 5b inset). Bending has been performed one time for each radius, with the sensor on the outer side of the bending curvature (tensile strain). Hall measurements have been performed afterwards in flat status in constant voltage mode. In addition to the measurements with different bending radii, the sensors have undergone up to 1000 bending cycles with a bending radius of 6.4 mm (Fig. 5b). No major degradation of the device performance is observed up to 1000 bending cycles. These results expand the application space of Hall sensors to flexible electronics, *e.g.*, wearable sensors for personal fitness or healthcare systems.

Conclusion

In summary, we have introduced the concept of tunable graphene Hall sensors through AC modulated gate voltages and performed an in-depth characterization of the devices. The AC top gate modulation increased the Hall signal, and thus the voltage and current normalized sensitivities, by a factor of ~2 compared to Hall sensors under DC operation. In addition, AC gate modulation enables read out of the sensors at kHz frequencies, where the noise level is significantly (by a factor of ~10^5) lower compared to the DC case and thus allows detecting much smaller magnetic fields (~10^2 higher magnetic resolution). In addition, the device concept and the fabrication process are compatible with large-scale flexible substrates. The performance does not degrade under bending and strain, which enables highly sensitive flexible Hall sensors. These results set a new benchmark for flexible Hall-sensors.

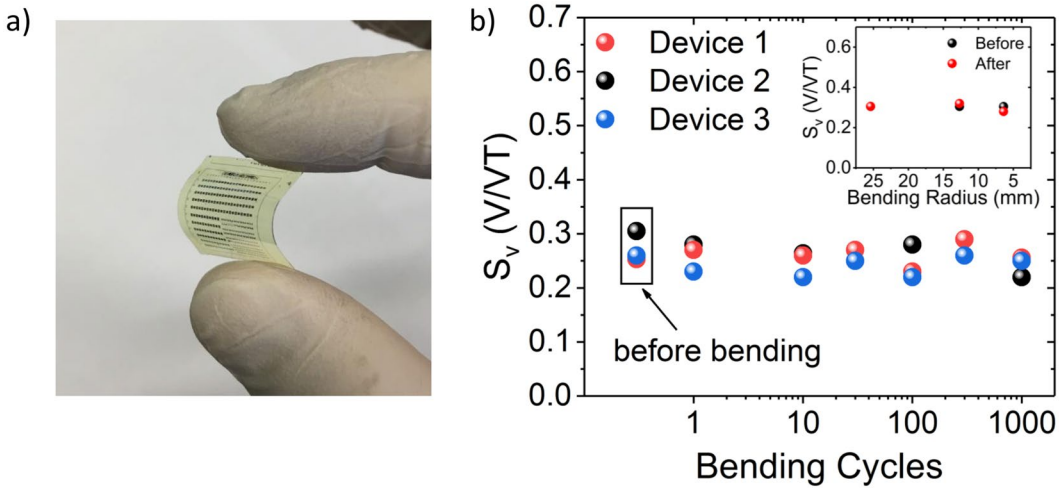

Figure 5. Bending tests for flexible Hall sensor. (**a**) Optical photograph of the flexible chip after it has been peeled off from Si substrate. (**b**) Bending cycle dependent measurement of the Hall sensor sensitivity. The PI substrate has been bent under bending radii of 6.4 mm up to 1000 times. The inset shows the measured S_v before and after bending tests with different bending radii of 25.4 mm, 12.7 mm, and 6.4 mm. The measurements have been carried out in flat status before and after bending at constant V_C of 300 mV and V_G of −1.2 V.

Methods

Graphene-based Hall sensors are fabricated on spin-coated PI substrate with conventional photolithography technology. First, the flexible substrates are prepared by spin-coating PI in liquid form on a silicon handling substrate. After curing, the resulting thickness of the solidified PI film is about 8 µm. During the entire fabrication process, Si is used as a supportive layer for the PI. After the PI substrate preparation, commercially available, large area, chemical vapor deposited graphene is transferred by a PMMA assisted method[28]. Graphene is patterned by oxygen plasma, and contacts to graphene are fabricated by sputtering 50 nm Ni, followed by a lift-off process. The top gate dielectric consists of 40 nm Al_2O_3 deposited by atomic layer deposition and the top-gate electrode is fabricated by sputter deposition of 20/500 nm Ti/Al and lift-off. Wet buffered oxide etchant is used to open vias in the Al_2O_3 to access the contacts. All measurements have been performed under ambient condition at room temperature. The devices have been measured in flat status with the PI still on silicon, but the entire flexible stack has been peeled off mechanically from the silicon carrier substrate for electric characterization under bending.

Received: 9 July 2019; Accepted: 1 November 2019;
Published online: 02 December 2019

References

1. R S Popovic. *Hall Effect Devices*. (IOP Publishing, 2004).
2. Marketsandmarkets.com. Magnetic Field Sensors Market by Type, Technology, Applications and Geography - Forecasts & Analysis to 2015–2021. *Mark. Mark. Rep* (2015).
3. Heremans, J. Solid state magnetic field sensors and applications. *J. Phys. D. Appl. Phys.* **26**, 1149–1168 (1993).
4. Kunets, V. P. *et al*. Highly sensitive micro-Hall devices based on Al0.12In0.88SbInSb heterostructures. *J. Appl. Phys*. **98** (2005).
5. Boero, G., Demierre, M., Besse, P.-A. & Popovic, R. S. Micro-Hall devices: performance, technologies and applications. *Sensors Actuators A Phys.* **106**, 314–320 (2003).
6. Bando, M. *et al*. High sensitivity and multifunctional micro-Hall sensors fabricated using InAlSb/InAsSb/InAlSb heterostructures. *J. Appl. Phys*. **105** (2009).
7. Shibasaki, I. Mass production of InAs Hall elements by MBE. *J. Cryst. Growth* **175–176**, 13–21 (1997).
8. Wang, Z., Shaygan, M., Otto, M., Schall, D. & Neumaier, D. Flexible Hall sensors based on graphene. *Nanoscale* **8**, 7683–7687 (2016).
9. Dauber, J. *et al*. Ultra-sensitive Hall sensors based on graphene encapsulated in hexagonal boron nitride. *Appl. Phys. Lett*. **106** (2015).
10. Huang, L. *et al*. Graphene/Si CMOS Hybrid hall integrated circuits. *Sci. Rep*. **4** (2014).
11. Berus, T., Oszwaldowski, M. & Grabowski, J. High quality Hall sensors made of heavily doped n-InSb epitaxial films. *Sensors Actuators, A Phys.* **116**, 75–78 (2004).
12. Koseva, R., Mönch, I., Schumann, J., Arndt, K. F. & Schmidt, O. G. Bismuth Hall probes: Preparation, properties and application. *Thin Solid Films* **518**, 4847–4851 (2010).
13. Hara, T., Mihara, M., Toyoda, N. & Zama, M. Highly Linear Gaas Hall Devices Fabricated By Ion Implantation. *IEEE Trans. Electron Devices* **29**, 78–82 (1982).
14. Banszerus, L. *et al*. Ultrahigh-mobility graphene devices from chemical vapor deposition on reusable copper. *Sci. Adv*. **1** (2015).
15. Huang, L. *et al*. Ultra-sensitive graphene Hall elements. *Appl. Phys. Lett*. **104** (2014).
16. Liang, Y. *et al*. High mobility flexible graphene field-effect transistors and ambipolar radio-frequency circuits. *Nanoscale* **7**, 10954–10962 (2015).
17. Polat, E. O. *et al*. Synthesis of Large Area Graphene for High Performance in Flexible Optoelectronic Devices. *Sci. Rep*. **5** (2015).
18. Polat, E. O. *et al*. Graphene-Enabled Optoelectronics on Paper. *ACS Photonics* **3**, 964–971 (2016).
19. Salihoglu, O. *et al*. Graphene-Based Adaptive Thermal Camouflage. *Nano Lett*. **18**, 4541–4548 (2018).
20. Schmitz, M. *et al*. High mobility dry-transferred CVD bilayer graphene. *Appl. Phys. Lett*. **110** (2017).
21. Wang, Z. *et al*. Flexible One-Dimensional Metal–Insulator–Graphene Diode. *ACS Appl. Electron. Mater*. acsaelm.9b00122, https://doi.org/10.1021/acsaelm.9b00122 (2019).

22. Wang, Z. *et al*. Encapsulated graphene-based Hall sensors on foil with increased sensitivity. *Phys. Status Solidi Basic Res.* **253**, 2316–2320 (2016).
23. Monch, I. J. *et al*. Flexible hall sensorics for flux-based control of magnetic levitation. *IEEE Trans. Magn*. **51** (2015).
24. Bolshakova, I. *et al*. Graphene and prospects of radiation-hard hall sensors. *Proc. 2017 IEEE 7th Int. Conf. Nanomater. Appl. Prop. N. 2017*, **2017-Janua**, 3–7 (2017).
25. Mosser, V., Matringe, N. & Haddab, Y. A Spinning Current Circuit for Hall Measurements Down to the Nanotesla Range. *IEEE Trans. Instrum. Meas.* **66**, 637–650 (2017).
26. Kang, C. G. *et al*. Mechanism of the effects of low temperature Al2O3 passivation on graphene field effect transistors. *Carbon N. Y.* **53**, 182–187 (2013).
27. Mavredakis, N., Garcia Cortadella, R., Bonaccini Calia, A., Garrido, J. A. & Jiménez, D. Understanding the bias dependence of low frequency noise in single layer graphene FETs. *Nanoscale* **10**, 14947–14956 (2018).
28. Suk, J. W. *et al*. Transfer of CVD-grown monolayer graphene onto arbitrary substrates. *ACS Nano* **5**, 6916–6924 (2011).
29. Vervaeke, K., Simoen, E., Borghs, G. & Moshchalkov, V. V. Size dependence of microscopic Hall sensor detection limits. *Rev. Sci. Instrum*. **80** (2009).
30. Xu, H. *et al*. Flicker noise and magnetic resolution of graphene hall sensors at low frequency. *Appl. Phys. Lett*. **103** (2013).
31. Melzer, M. *et al*. Wearable magnetic field sensors for flexible electronics. *Adv. Mater.* **27**, 1274–1280 (2015).

Acknowledgements

This work was financially supported by the European Commission under the project Graphene Flagship (contract no. 785219) and by the German Science Foundation (DFG) within the priority program FFlexCom Project "GLECS" (contract no. NE1633/3).

Author contributions

B.U. and D.N. proposed the idea and planned the experiments. M.O. helped for sample preparation. B.U. fabricated the devices and performed all the experiments. Z.W. and S.L. helped for the measurements. B.U. analyzed the data and wrote the manuscript. The manuscript was critically reviewed by M.C.L. and D.N. All authors reviewed the manuscript and approved the final version of the manuscript.

Competing interests

The authors declare no competing interests.

Additional information

Supplementary information is available for this paper at https://doi.org/10.1038/s41598-019-54489-0.

Correspondence and requests for materials should be addressed to B.U.

Reprints and permissions information is available at www.nature.com/reprints.

Publisher's note Springer Nature remains neutral with regard to jurisdictional claims in published maps and institutional affiliations.